Mixed-Symmetry 2^+ State of ^{56}Fe in Realistic Shell Model

Hitoshi Nakada
Physics Laboratory, Juntendo University, Inba-mura, Inba-gun, Chiba 270-16, Japan

Takaharu Otsuka
Department of Physics, University of Tokyo, Hongo, Bunkyo-ku, Tokyo 113, Japan

Takashi Sebe
College of Engineering, Hosei University, Koganei, Tokyo 184, Japan

(Received 5 February 1991)

The mixed-symmetry 2^+ state of ^{56}Fe is investigated by a large-scale shell-model calculation. We can reproduce the experimental energy levels by the Kuo-Brown interaction, as well as the $E2$ and $M1$ transition probabilities. The (e,e') form factors are also reproduced by including the core-polarization effect. By inspecting the shell-model wave functions thus tested, it is found that the 2_2^+ and 2_4^+ states share a large fraction of the mixed-symmetry component.

PACS numbers: 21.60.Cs, 21.10.Re, 25.30.Dh, 27.40.+z

The interacting boson model (IBM) [1] has been successful in the description of lowest collective states which are predominantly symmetric with respect to the proton and neutron degrees of freedom. On the other hand, in the proton-neutron interacting boson model (IBM-2) [2,3], mixed-symmetry states have been predicted at higher excitation energies. The lowest mixed-symmetry 1^+ state corresponds to the scissors mode [4,5]. For vibrational nuclei, the mixed-symmetry 2^+ state has been predicted since the IBM-2 was founded [3]. This state is interpreted as a quadrupole surface oscillation out of phase between protons and neutrons. Despite some earlier studies [6], the mixed-symmetry 2^+ state has not been confirmed so far. In this Letter we shall search for a mixed-symmetry 2^+ state in ^{56}Fe by performing a large-scale shell-model calculation with an interaction derived from the G matrix. The shell-model calculation is required to yield precise wave functions which are needed to study the mixed-symmetry 2^+ state. ^{56}Fe provides us with a meeting point of the realistic shell-model calculation and the quadrupole collectivity; the former has practical limits for increasing particle number, whereas the latter appears only in heavier nuclei. Thus ^{56}Fe gives a precious testing ground to understand the mixed-symmetry states.

Eid *et al.* claimed that the 2_2^+ and 2_3^+ states share the mixed-symmetry component in ^{56}Fe, based on the relatively large observed $B(M1)$ values from these states to 2_1^+ [7]. Moreover, Hartung *et al.* showed that the (e,e') form factors can be described consistently with the above interpretation to a certain extent [8]. The wave functions used in these studies, however, do not seem to be sufficiently accurate, and indeed cause various difficulties as will be discussed later. More reliable wave functions are needed in order to investigate the mixed-symmetry 2^+ state.

We study the mixed-symmetry problem of ^{56}Fe by a shell-model calculation. Assuming ^{40}Ca to be a doubly magic inert core, we consider the following configurations:

$$(0f_{7/2})^{14-k}(0f_{5/2}1p_{3/2}1p_{1/2})^{2+k}. \qquad (1)$$

While $k=0$ gives the configuration in which excitation across N or $Z=28$ is absent, we shall use the model space containing all configurations of $k=0$, 1, and 2. The description of ^{56}Fe with only the $k=0$ configuration [9] or that with the $k=0$ and 1 configurations [10] fail to reproduce the properties of the 2^+ states higher than 2_2^+. For instance, the shell-model calculation in Ref. [9] overestimates the excitation energy of 2_3^+ by 0.4 MeV and of 2_4^+ by 0.5 MeV. Therefore, the $k=2$ configuration is crucial.

As for the effective Hamiltonian, we adopt the Kuo-Brown Hamiltonian [11]. The single-particle energies are determined from experimental data of one-particle states on the top of the ^{40}Ca core. The two-body interaction is obtained from the G matrix derived from the Hamada-Johnston potential, including three-particle–one-hole (3p-1h) corrections. Thus there are no adjustable parameters in the calculation of energy levels. The isospin is conserved, and hereafter we restrict ourselves to the $T=2$ states.

The experimental and calculated energy levels are shown in Fig. 1. The experimental spectrum is excellently reproduced for $E_x < 4$ MeV. Discrepancies are typically around only 0.1 MeV. The $k=0$ configuration is dominant in most of the displayed eigenstates with (50–60)% probability, but even the ground state contains as much as 27% $k=2$ configuration.

The $B(E2)$ and $B(M1)$ values are exhibited in Table I, as well as the $E2$ and $M1$ moments of the 2_1^+ state. We use the $E2$ operator

$$T(E2)=\sum_{\rho=\pi,\nu} e_\rho^{\text{eff}} Q_\rho\,, \qquad (2)$$

where $Q_\rho=[r^2Y^{(2)}]_\rho$, with effective charges $e_\pi^{\text{eff}}=1.4e$ and $e_\nu^{\text{eff}}=0.9e$. We assume the single-particle wave functions in the harmonic-oscillator potential, with oscillator length $b=A^{1/6}=1.956$ fm. The $M1$ operator is

$$T(M1)=\left(\frac{3}{4\pi}\right)^{1/2}\sum_{\rho=\pi,\nu}(g_{l,\rho}^{\text{eff}}L_\rho+g_{s,\rho}^{\text{eff}}S_\rho)\,, \qquad (3)$$

where L_ρ and S_ρ denote orbital and spin angular momen-

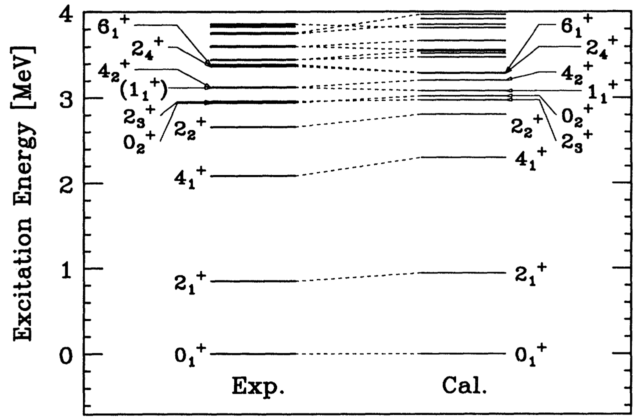

FIG. 1. Energy levels of positive-parity states of ^{56}Fe with $E_x < 4$ MeV.

tum operators, respectively. Single-particle g factors $g_{l,\pi}^{\rm eff}=1.0$, $g_{l,\nu}^{\rm eff}=0.0$, $g_{s,\pi}^{\rm eff}=0.5g_{s,\pi}^{\rm free}$, and $g_{s,\nu}^{\rm eff}=0.5g_{s,\nu}^{\rm free}$ are adopted, where $g_{s,\rho}^{\rm free}$ denotes the free nucleon values. The electromagnetic properties are reproduced well, except for $B(M1;2_3^+\to 2_1^+)$, which is a noncollective transition as will be mentioned later. This reproduction of the electromagnetic properties as well as the energy levels indicates the reliability of the wave functions.

Now we turn to the mixed-symmetry 2^+ components in the wave functions. For this purpose we consider S and D pairs, which correspond to the s and d bosons in the IBM [2]. If we assume the $N=Z=28$ doubly magic core, ^{56}Fe has a pair of proton holes and a pair of neutron valence particles. Within the $k=0$ configuration in Eq. (1), S and D pairs of protons are defined as the 0^+ and 2^+ states of the $(0f_{7/2})^{-2}$ configuration, while those of neutrons are collective 0^+ and 2^+ states of the $(0f_{5/2}1p_{3/2}1p_{1/2})^2$ configuration. The complete set of the 2^+ states within the SD space is spanned by

$$\begin{aligned}|2_S^+(SD)\rangle\rangle &= (1/\sqrt{2})(|S_\pi\rangle\otimes|D_\nu\rangle+|D_\pi\rangle\otimes|S_\nu\rangle)\,,\\ |2_S^+(D^2)\rangle\rangle &= [|D_\pi\rangle\otimes|D_\nu\rangle]^{(2)}\,,\\ |2_M^+(SD)\rangle\rangle &= (1/\sqrt{2})(|S_\pi\rangle\otimes|D_\nu\rangle-|D_\pi\rangle\otimes|S_\nu\rangle)\,.\end{aligned} \tag{4}$$

Obviously the first two states correspond to the totally symmetric states in the IBM-2 after the Otsuka-Arima-Iachello (OAI) mapping [2], whereas the last corresponds to the mixed-symmetry state. Recently Halse investigated the wave functions of Ref. [9] from this viewpoint [13] and found that the 0_1^+ and 2_1^+ states are totally symmetric states to a good approximation, while 2_2^+ has quite a large fraction (~80%) of the mixed-symmetry state. However, the present wave functions contain a considerable amount of $k>0$ configurations. In order to take this effect into account, we extend the SD pair states.

The wave functions of ^{56}Fe are expanded in terms of products of proton and neutron wave functions as

$$|\Psi(\sigma)\rangle\rangle = \sum_{\sigma',\sigma''} c^{\sigma}_{\sigma',\sigma''}|\varphi_\pi(\sigma')\rangle\rangle\otimes|\varphi_\nu(\sigma'')\rangle\rangle\,, \tag{5}$$

TABLE I. Electromagnetic properties of low-lying 2^+ states of ^{56}Fe: The upper box exhibits $B(E2)$ values (e^2fm^4), while the lower box shows $B(M1)$ (μ_N^2, where μ_N is nuclear magneton). In the diagonal case, the $E2$ or $M1$ static moment ($e$fm^2 or μ_N) is displayed. Experimental data are taken from Ref. [12].

Initial	Final	$B(E2)$ (Calc.)	$B(E2)$ (Expt.)
2_1^+	0_1^+	213.1	214 ± 8
2_2^+	0_1^+	5.1	6^{+8}_{-6}
2_3^+	0_1^+	0.6	1.0 ± 0.1
2_4^+	0_1^+	15.5	10 ± 5
2_1^+	2_1^+	-28.8[a]	-23 ± 3[a]
Initial	**Final**	**$B(M1)$ (Calc.)**	**$B(M1)$ (Expt.)**
2_1^+	2_1^+	1.17[b]	1.2 ± 0.2[b]
2_2^+	2_1^+	0.28	0.23 ± 0.07
2_3^+	2_1^+	0.00	0.07 ± 0.01
2_4^+	2_1^+	0.13	0.11 ± 0.05

[a]Quadrupole moment. [b]Magnetic moment.

where the $c^{\sigma}_{\sigma',\sigma''}$ stand for expansion coefficients, and the σ's specify the states in each space. The proton [neutron] basis states $|\varphi_\pi(\sigma)\rangle\rangle$ [$|\varphi_\nu(\sigma)\rangle\rangle$] are taken to be eigenstates of the corresponding single-closed system. By using the $|\varphi_\rho(\sigma)\rangle\rangle$ bases, we define the extended SD states ($\rho=\pi,\nu$),

$$|\tilde{S}_\rho\rangle = \sum_i x_{i,\rho}^{(0)}|\varphi_\rho(0_i^+)\rangle\rangle,\quad |\tilde{D}_\rho\rangle = \sum_i x_{i,\rho}^{(2)}|\varphi_\rho(2_i^+)\rangle\rangle\,, \tag{6}$$

by an optimization procedure described below. The coefficients $x_{i,\rho}^{(0)}$ are determined so that the overlap between the product state $|\tilde{S}_\pi\rangle\otimes|\tilde{S}_\nu\rangle$ and the ground state of ^{56}Fe should be maximum. Following this step, $x_{i,\pi}^{(2)}$ are determined by maximizing the overlap between $|\tilde{D}_\pi\rangle\otimes|\tilde{S}_\nu\rangle$ and the 2_1^+ state of ^{56}Fe, while $x_{i,\nu}^{(2)}$ are determined from the overlap between $|\tilde{S}_\pi\rangle\otimes|\tilde{D}_\nu\rangle$ and 2_1^+ of ^{56}Fe. In these optimizations we used about twenty $|\varphi_\rho(J_i^+)\rangle\rangle$ bases for each ρ ($=\pi,\nu$) and J, confirming the convergence. In the resultant $|\tilde{S}_\pi\rangle$ ($|\tilde{D}_\pi\rangle$) state the weight of the $(0f_{7/2})^{-2}$ configuration is 84% (78%), while in the $|\tilde{S}_\nu\rangle$ ($|\tilde{D}_\nu\rangle$) state the weight of the $(0f_{5/2}1p_{3/2}1p_{1/2})^2$ configuration is 89% (85%). This procedure would lead to a possible generalization of the OAI mapping [2], by connecting these $\tilde{S}\tilde{D}$ states to sd boson states.

Table II shows overlaps between the $\tilde{S}\tilde{D}$ product states and some eigenstates of ^{56}Fe. The 0_1^+ state is an almost pure $\tilde{S}\tilde{D}$ state. The 2_1^+ state is primarily in the $\tilde{S}\tilde{D}$ subspace, and has almost equal amplitudes for the $|\tilde{S}_\pi\rangle\otimes|\tilde{D}_\nu\rangle$ and $|\tilde{D}_\pi\rangle\otimes|\tilde{S}_\nu\rangle$ components, which is consistent with the totally symmetric nature. On the other hand, the amounts of $|\tilde{S}_\pi\rangle\otimes|\tilde{D}_\nu\rangle$ and $|\tilde{D}_\pi\rangle\otimes|\tilde{S}_\nu\rangle$ components in the 2_2^+ state are large and close to each other, but the signs of the amplitudes are opposite. A similar situation is found for 2_4^+. Thus the 2_2^+ and 2_4^+ states share the mixed-symmetry component. It should be emphasized that about half of the mixed-symmetry component is concentrated in these two states, which are around $E_x=3$

TABLE II. Overlaps between $\tilde{S}\tilde{D}$ states and eigenstates of ^{56}Fe.

State	$\lvert\tilde{S}_\pi\rangle\otimes\lvert\tilde{S}_\nu\rangle$	$\lvert\tilde{S}_\pi\rangle\otimes\lvert\tilde{D}_\nu\rangle$	$\lvert\tilde{D}_\pi\rangle\otimes\lvert\tilde{S}_\nu\rangle$	$[\lvert\tilde{D}_\pi\rangle\otimes\lvert\tilde{D}_\nu\rangle]^{(J)}$	$\tilde{S}\tilde{D}$ prob.
0_1^+	0.74			0.53	83%
2_1^+		0.55	0.56	0.37	74%
2_2^+		0.38	−0.35	−0.09	27%
2_3^+		0.10	0.03	−0.09	2%
2_4^+		0.27	−0.26	0.09	15%

MeV. In the other 2^+ states with $E_x < 5$ MeV, the admixture of the mixed-symmetry component is only a few percent in total. The remaining fraction of the mixed-symmetry component goes to much higher energy or is highly fragmented. It is found that the state generated from $(1/\sqrt{2})(\lvert\tilde{S}_\pi\rangle\otimes\lvert\tilde{D}_\nu\rangle - \lvert\tilde{D}_\pi\rangle\otimes\lvert\tilde{S}_\nu\rangle)$ by orthogonalizing to the 2^+ states with $E_x < 5$ MeV is distributed, with the centroid at $E_x = 10.4$ MeV. The present realistic interaction hardly mixes a symmetric state $[\lvert\tilde{D}_\pi\rangle\otimes\lvert\tilde{D}_\nu\rangle]^{(2)}$ into 2_2^+ or 2_4^+. Namely, the realistic interaction seems to conserve the F-spin-like symmetry in this nucleus. Thus the mixed-symmetry 2^+ state appears as a basic mode, and 2_2^+ and 2_4^+ share this mode in ^{56}Fe, contrary to the previous report in Refs. [7,8]. Note that, although the $\tilde{S}\tilde{D}$ product states do not necessarily have good isospin, the leakage out of the $T=2$ space is only a few percent.

The fragmentation of the mixed-symmetry 2^+ component into the 2_2^+ and 2_4^+ states comes from mixing with states outside the $\tilde{S}\tilde{D}$ space. Because of the mixing, the matrix elements $\langle 2_2^+ \| Q_\rho \| 0_1^+\rangle$ and $\langle 2_4^+ \| Q_\rho \| 0_1^+\rangle$ ($\rho = \pi, \nu$) contain $\tilde{S}\tilde{D}$ and non-$\tilde{S}\tilde{D}$ contributions in similar magnitudes.

The 2_3^+ state is an entirely noncollective state. It is confirmed that about half of this state is a product of the $\tilde{S}_\pi$ and a neutron noncollective 2^+ state.

The J_π and J_ν operators, where $J_\rho = L_\rho + S_\rho$ ($\rho = \pi, \nu$), are alternative devices to discuss the proton-neutron symmetry [14]. We obtain results consistent with those of the $\tilde{S}\tilde{D}$ decomposition.

In order to confirm the conclusions obtained above, we calculate (e,e') form factors from the ground state to several 2^+ states. The method of Sagawa and Brown [15] is employed for this calculation. Single-particle wave functions are obtained by the Hartree-Fock (HF) method with the SGII Skyrme interaction [16], and isoscalar (IS) and isovector (IV) giant quadrupole resonances (GQR) are obtained by the random-phase approximation (RPA). The core-polarization effect caused by the GQR is incorporated into the single-particle wave functions with the mixing amplitudes evaluated in perturbation theory. In this process, we take into account one IS GQR peak at $E_x \simeq 17$ MeV, which is completely isolated, and nine typical IV GQR peaks among the many peaks distributed over $E_x = 20$–35 MeV. In the RPA and the perturbative calculation, the residual particle-hole interaction is derived from the SGII interaction, consistently with the HF calculation. With the renormalized single-particle wave functions around the ^{56}Ni core, the $C2$ form factors are calculated from the shell-model density matrices. This calculation again contains no adjustable parameter. The results are shown in Fig. 2, in comparison with experimental data taken from Refs. [8,17,18], in which the transverse mode was not separated. The form factors of the excitation to the 2_1^+ and 2_2^+ states are in remarkable agreement. Though there are only few data points for 2_4^+, we can reproduce the order of magnitude of the first peak, which is higher than those of 2_2^+ and 2_3^+, reflecting the collectivity. The difference between 2_2^+ and 2_4^+ arises from the coupling to degrees of freedom outside the $\tilde{S}\tilde{D}$ space. The form factor to 2_3^+ is not reproduced so well. This could be related to the small collectivity of the state. It is not so evident if the method of Sagawa and Brown is applicable to such a noncollective transition. Note that, in reproducing the form factors to the 2_1^+, 2_2^+, and 2_3^+ states, Hartung *et al.* [8] utilized state-dependent normalization factors (0.2–2), in addition to effective charges [19]. The magnitude of the form factor to the 2_4^+ state relative to the other 2^+ states is not reproduced by the wave function in Ref. [13], while 2_4^+ is out of consideration in Ref. [8].

In Ref. [20], $(\vec{p},p')$ data at $E_p = 65$ MeV have been analyzed by the distorted-wave Born approximation with the present shell-model density matrices. The differential

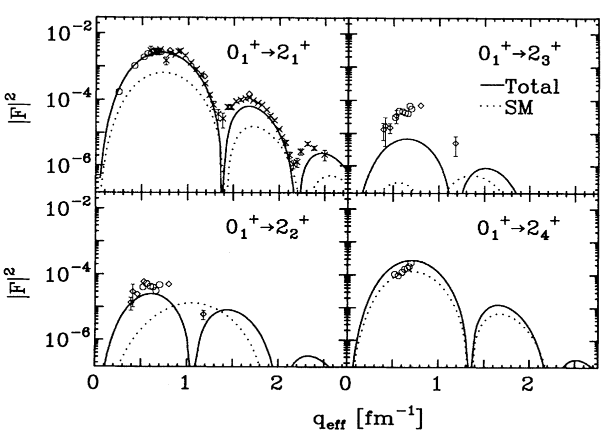

FIG. 2. Transition form factors from the ground state to the lowest four 2^+ states of ^{56}Fe. Solid lined display Coulomb form factors calculated by the shell model with the core-polarization effect. Those without core polarization are shown by dotted lines. Circles, crosses, and diamonds exhibit experimental data taken from Refs. [17], [18], and [8], respectively.

cross sections have been reproduced for the excitations to the 2_1^+, 2_2^+, and 2_4^+ states with much better agreement than by using the wave functions of Ref. [8]. The excitation to the 2_3^+ state shows a strikingly anomalous angular distribution. The present shell-model wave function reproduces this anomaly, while the wave function of Ref. [8] cannot. Therefore this angular distribution also indicates the noncollective character of 2_3^+. The validity of our wave functions can be thus confirmed by the (e,e') and $(\vec{p},p')$ data.

In summary, the properties of low-lying 2^+ states of ^{56}Fe have been described by a large-scale shell-model calculation with a realistic interaction. The present shell-model wave functions have been stringently tested by calculating various physical observables, such as energy levels, electromagnetic properties, (e,e') form factors, and $(\vec{p},p')$ differential cross sections. By inspecting the wave functions, the 2_2^+ and 2_4^+ states are found to share the mixed-symmetry component, while 2_3^+ is an entirely noncollective state. It is a notable consequence that the mixed-symmetry 2^+ component in the lower-energy region ($E_x < 5$ MeV) is concentrated on only two states, although there are about ten 2^+ states in this region. This result is not trivial in a realistic treatment like the present one, whereas the mixed-symmetry state naturally keeps the purity in calculations using a restricted model space as in Ref. [13]. We also find that the F-spin-like symmetry is conserved remarkably well by the G-matrix interaction.

The authors are grateful to Dr. K. Ogawa and to Dr. H. Sagawa for useful discussions. The authors thank Dr. M. Fujiwara and Dr. J. Takamatsu for informing them of the $(\vec{p},p')$ results. The authors also thank Dr. W. Bentz for careful reading of the manuscript. The numerical calculation has been partly carried out by HITAC S-820/80 in Kanagawa Factory, Hitachi Corporation. This work has been financially supported in part by the Grant-in-Aid for General Scientific Research (No. 01540231) by the Ministry of Education, Science and Culture, as well as by Research Center of Nuclear Physics, Osaka University.

[1] F. Iachello and A. Arima, *The Interacting Boson Model* (Cambridge Univ. Press, New York, 1987).
[2] T. Otsuka, A. Arima, and F. Iachello, Nucl. Phys. **A309**, 1 (1978).
[3] T. Otsuka, Ph.D. thesis, University of Tokyo, 1979 (unpublished).
[4] F. Iachello, Nucl. Phys. **A358**, 89c (1981).
[5] A. Richter, Nucl. Phys. **A522**, 139c (1991).
[6] F. Iachello, Phys. Rev. Lett. **53**, 1427 (1984); T. Otsuka and J. N. Ginocchio, Phys. Rev. Lett. **54**, 777 (1985); W. D. Hamilton *et al.*, Phys. Rev. Lett. **53**, 2469 (1984); M. Pignanelli *et al.*, Phys. Lett. B **202**, 470 (1988); R. de Leo *et al.*, Phys. Lett. B **226**, 5 (1989).
[7] S. A. A. Eid *et al.*, Phys. Lett. **166B**, 267 (1986); S. P. Collins *et al.*, J. Phys. G **15**, 321 (1989).
[8] G. Hartung *et al.*, Phys. Lett. B **221**, 109 (1989).
[9] H. Horie and K. Ogawa, Nucl. Phys. **A216**, 407 (1973).
[10] R. B. M. Mooy and P. W. M. Glaudemans, Z. Phys. A **312**, 59 (1983).
[11] T. T. S. Kuo and G. E. Brown, Nucl. Phys. **A114**, 241 (1968).
[12] H. Junde *et al.*, Nucl. Data Sheets **51**, 1 (1987).
[13] P. Halse, Phys. Rev. C **41**, 2340 (1990).
[14] T. Otsuka, in *Understanding the Variety of Nuclear Excitations*, edited by A. Covello (World Scientific, Singapore, 1991).
[15] H. Sagawa and B. A. Brown, Nucl. Phys. **A430**, 84 (1984).
[16] N. van Giai and H. Sagawa, Nucl. Phys. **A371**, 1 (1981).
[17] R. J. Peterson *et al.*, Nucl. Phys. **A153**, 610 (1970).
[18] J. Heisenberg *et al.*, Nucl. Phys. **A164**, 353 (1971).
[19] A. Richter (private communication).
[20] J. Takamatsu *et al.*, J. Phys. (Paris), Colloq. **51**, C6-423 (1990).